Acta Pharmacologica Sinica

ARTICLE

Gout-associated monosodium urate crystal-induced necrosis is independent of NLRP3 activity but can be suppressed by combined inhibitors for multiple signaling pathways

Chun-su Zhong[1], Bo Zeng[1], Jia-hao Qiu[1], Li-hui Xu[2], Mei-yan Zhong[1], Yuan-ting Huang[1], Rong Xu[1], Si-ying Liu[1], Qing-bing Zha[3], Bo Hu[4], Dong-yun Ou-Yang[1] and Xian-hui He[1]

Monosodium urate (MSU) crystals, the etiological agent of gout, are formed in joints and periarticular tissues due to long-lasting hyperuricemia. Although MSU crystal-triggered NLRP3 inflammasome activation and interleukin 1β (IL-1β) release are known to have key roles in gouty arthritis, recent studies revealed that MSU crystal-induced necrosis also plays a critical role in this process. However, it remains unknown what forms of necrosis have been induced and whether combined cell death inhibitors can block such necrosis. Here, we showed that MSU crystal-induced necrosis in murine macrophages was not dependent on NLRP3 inflammasome activation, as neither genetic deletion nor pharmacological blockade of the NLRP3 pathway inhibited the necrosis. Although many cell death pathways (such as ferroptosis and pyroptosis) inhibitors or reactive oxygen species inhibitors did not have any suppressive effects, necroptosis pathway inhibitors GSK′872 (RIPK3 inhibitor), and GW806742X (MLKL inhibitor) dose-dependently inhibited MSU crystal-induced necrosis. Moreover, a triple combination of GSK′872, GW806742X, and IDN-6556 (pan-caspase inhibitor) displayed enhanced inhibition of the necrosis, which was further fortified by the addition of MCC950 (NLRP3 inhibitor), suggesting that multiple cell death pathways might have been triggered by MSU crystals. Baicalin, a previously identified inhibitor of NLRP3, inhibited MSU crystal-induced inflammasome activation and suppressed the necrosis in macrophages. Besides, baicalin gavage significantly ameliorated MSU crystal-induced peritonitis in mice. Altogether, our data indicate that MSU crystals induce NLRP3-independent necrosis, which can be inhibited by combined inhibitors for multiple signaling pathways, highlighting a new avenue for the treatment of gouty arthritis.

Keywords: monosodium urate crystals; regulated necrosis; necroptosis; inflammasome; baicalin

Acta Pharmacologica Sinica (2022) 43:1324–1336; https://doi.org/10.1038/s41401-021-00749-7

INTRODUCTION

Gout is a common type of inflammatory arthritis in human adults [1], which is caused by the deposition of monosodium urate (MSU) crystals in joints and periarticular tissues due to long-lasting hyperuricemia [2–4]. Although MSU crystals had already been identified, as the etiological agent of gout in the 18th century, it was in the first decade of the 21st century, that MSU crystals were shown to be an activator of NLRP3 inflammasome in innate immune cells including macrophages [5]. MSU crystal-induced activation of NLRP3 inflammasome results in the generation of active caspase-1, which in turn converts pro-IL-1β into mature IL-1β. The latter released from macrophages has potent pro-inflammatory activities, and thus play a critical role in the initiation and pathogenesis of gouty arthritis [2, 3]. Thus, blocking the biological activity of IL-1β represents an effective therapeutic regimen for the treatment of gouty arthritis [6].

Apart from mediating the inflammatory cytokine IL-1β maturation, active caspase-1 resulting from NLRP3 inflammasome activation can also cleave gasdermin D (GSDMD) to generate its N-terminal fragment (GSDMD-NT), that forms pores in the plasma membrane to execute pyroptosis [7–11], the latter of which is an inflammatory form of regulated cell death [12–14]. Consistent with their triggering of NLRP3 inflammasome assembly, MSU crystals can induce the generation of GSDMD-NT in macrophages, but genetic deletion of GSDMD did not prevent MSU crystal-induced necrosis [15]. Further studies showed that MSU crystal- or other particulate matter-induced necrosis in murine kidney epithelial cells is mediated by the receptor-interacting protein (RIP) kinase-1 (RIPK1), RIP kinase-3 (RIPK3), and pseudokinase mixed-lineage kinase domain-like (MLKL)-driven necroptotic pathway [16]. However, in mouse macrophages, genetic deletion of MLKL fails to prevent MSU crystal-induced necrosis [15], suggesting that cell-type-specific forms of cell death had been elicited in response to MSU crystal stimulation. Thus, what forms of regulated necrosis are induced by MSU crystals in macrophages remain unclear.

[1]Department of Immunobiology, College of Life Science and Technology, Jinan University, Guangzhou 510632, China; [2]Department of Cell Biology, College of Life Science and Technology, Jinan University, Guangzhou 510632, China; [3]Department of Fetal Medicine, The First Affiliated Hospital of Jinan University, Guangzhou 510630, China and [4]Department of Nephrology, The First Affiliated Hospital of Jinan University, Guangzhou 510630, China
Correspondence: Bo Hu (42089537@qq.com) or Dong-yun Ou-Yang (dongyun1967@aliyun.com) or Xian-hui He (thexh@jnu.edu.cn)
These authors contributed equally: Chun-su Zhong, Bo Zeng, Jia-hao Qiu.

Received: 3 April 2021 Accepted: 20 July 2021
Published online: 10 August 2021

It is worth noting that MSU crystals, as well as other particulate matters, are reported to elicit direct cytotoxic effects, inflammation, and inflammation-driven cell necrosis, in an auto-amplifying loop that is referred to as necroinflammation [4]. Consequently, blocking the inflammatory necrosis induced by MSU crystals would provide benefits for gout patients [4]. It is thus believed that regulated cell death, including regulated necrosis, can serve as a potential therapeutic target for various inflammatory diseases [17]. Yet there are currently no agents available to effectively block such necrosis. Previous studies showed that pan-caspase inhibitors (i.e., Z-VAD-fmk and IDN-6556), as well as cathepsin B inhibitor (e.g., CA-074-Me) did not inhibit MSU crystal-induced necrosis in either wild-type or MLKL-deficient murine macrophages [15]. Thus it remains to be explored whether inhibitors of other cell death signaling pathways could suppress MSU crystal-induced necrosis in macrophages.

Interestingly, recent studies revealed that murine macrophages can simultaneously undergo multiple forms of cell death, including pyroptosis, apoptosis, and necroptosis, in response to influenza A virus, vesicular stomatitis virus, *Listeria monocytogenes*, *Salmonella enterica serovar* Typhimurium, *Yersinia pseudotuberculosis,* or mouse hepatitis virus infections [18–20], which have been named PANoptosis [21, 22]. The multiple protein complexes that mediate PANoptosis have been called as PANoptosome [22]; importantly, combined deletion of PANoptotic components, including caspase-1/-11, RIPK3, and caspase-8, can largely prevent macrophages from necrosis induced by those pathogens, whereas deleting any one of them provides reduced or no protection [18]. In addition, it has been revealed that one form of cell death can be switched to another when one signaling pathway is blocked by pathogens or by artificial interventions [23–25]. We, therefore, proposed that MSU crystal-induced cell death likely contains multiple forms of regulated necrosis which can only be suppressed by a combination of inhibitors for multiple signaling pathways. To test this hypothesis, in this study, we had assayed various combinations of signaling pathway inhibitors and found that, indeed, MSU crystal-induced necrosis was not efficiently suppressed by a variety of individual inhibitors for different signaling pathways but was markedly blocked by a combined regimen of inhibitors. Our data also provided evidence that the natural product baicalin, which has previously been shown to have anti-inflammatory and anti-oxidative activities by others [26, 27], and has also been reported to inhibit NLRP3 inflammasome activation by us [28], could effectively inhibit MSU crystal-induced necrosis in vitro and mitigate MSU crystal-induced peritonitis in mice in vivo. These data highlight a new avenue for the treatment of gouty arthritis through a combination of cell death inhibitors to suppress MSU crystal-induced necrosis.

MATERIALS AND METHODS

Reagents and antibodies

Monosodium urate (MSU) crystals (tlrl-msu-25) and nigericin (tlrl-nig-5) were obtained from InvivoGen (San Diego, CA, USA). MSU crystals were resuspended in sterile phosphate-buffered saline (PBS) and stored at −20 °C. Baicalin (572667), propidium iodide (PI), Hoechst 33342, lipopolysaccharide (LPS) (*Escherichia coli* O111: B4) (L4391), disuccinimidyl suberate, phorbol 12-myristate 13-acetate (PMA), ATP (A6419), and dimethyl sulfoxide (DMSO) were bought from Sigma-Aldrich (St. Louis, MO, USA). GW806742X (HY-112292), disulfiram (HY-B0240), CA-074-Me (HY-100350), ferrostatin-1 (HY-100579), and cyclosporin A (HY-B0579) were purchased from MedChemExpress (Princeton, NJ, USA). IDN-6556 (S7775), GSK'872 (S8465), necrostatin-1 (S8037), E64d (S7393), MCC950 (S7809), and VX-765 (S2228) were obtained from Selleck Chemical (Houston, TX, USA). CytoTox 96 nonradioactive cytotoxicity assay kit was from Promega (Madison, WI, USA). Dulbecco's Modified Eagle's Medium (DMEM) with high glucose, RPMI-1640, β-mercaptoethanol, Opti-MEM, fetal bovine serum (FBS), streptomycin, and penicillin were bought from ThermoFisher (Carlsbad, CA, USA). Specific antibodies against IL-1β (#12242), β-actin (#3700), ASC AlexaFluor488-conjugated (#17507), horseradish peroxidase (HRP)-conjugated horse anti-mouse IgG (#7076), and HRP-conjugated goat-anti-rabbit IgG (#7074) were purchased from Cell Signaling Technology (Danvers, MA, USA). The antibody against NLRP3 (Cryo-2) (AG-20B-0014) was obtained from Adipogen AG (Liestal, Switzerland). Rabbit monoclonal antibodies against pro-caspase-1+p10+p12 (ab179515) and GSDMD (ab209845) were bought from Abcam (Cambridge, UK). CF568-conjugated goat-anti-rabbit IgG (#20103) was obtained from Biotium (Hayward, CA, USA). Anti-mouse CD11b FITC (#101205) and anti-mouse Ly-6G PE (#127607) were obtained from BioLegend (San Diego, CA, USA).

Animals

C57BL/6 J mice (6–8 weeks of age) were bought from the Laboratory Animal Center of Southern Medical University (Guangzhou, China). Mice were acclimatized for 1 week before experiments. C57BL/6 J *NLRP3*$^{+/-}$ mice were generated by CRISPR/Cas9 system from GemPharmatech Co. (Nanjing China) and the homozygote genotype was identified as previously described [29]. Both female and male *NLRP3*$^{-/-}$ mice were used in experiments. All animal experiments were performed according to the guidelines for the care and use of animals approved by the Committee on the Ethics of Animal Experiments of Jinan University.

Bone marrow-derived macrophages

Murine bone marrow-derived macrophages (BMDMs) were differentiated as described previously [30]. Briefly, C57BL/6 J mice were sacrificed and bone marrows were collected from the femurs. Collected bone marrow cells were differentiated in BMMAC medium (80% DMEM supplemented with 10% FBS and 1% penicillin and streptomycin plus 20% M-CSF-contained medium from L929 cells) for 6 days at 37 °C in a humidified incubator of 5% CO_2.

THP-1-derived macrophages

Human THP-1 cells (kindly provided by Dr. Yao Wang at Sun Yat-sen University, Guangzhou) were cultured in RPMI-1640 supplemented with 10% FBS, 1% penicillin, and streptomycin, and 50 μM β-mercaptoethanol, at 37 °C in a humidified incubator with 5% CO_2. THP-1 cells were differentiated into macrophages by incubation with 100 nM of PMA for 16 h, which was ready for experiments.

Lytic cell death assay

Cell death was measured by propidium iodide (PI) incorporation as reported previously [31, 32]. In brief, cells were cultured in 24-well plates at 2.5×10^5 cells/well (0.5 mL) with the complete medium (DMEM containing 10% FBS and 1% penicillin and streptomycin) at 37 °C overnight and primed with 1 μg/mL LPS in Opti-MEM for 4 h. The cells were then pre-treated with or without indicated concentrations of inhibitors for 1 h followed by treatment with MSU crystals (300 μg/mL) in Opti-MEM for 6 h. The cells were stained with staining solution (2 μg/mL PI and 5 μg/mL Hoechst 33342 in PBS) for 10 min at room temperature and observed immediately by live imaging using Zeiss Axio Observer D1 microscope (Carl Zeiss, Göttingen, Germany). Fluorescence images were captured with a Zeiss AxioCam MR R3 cooled CCD camera controlled with ZEN software (Carl Zeiss).

Immunofluorescence microscopy

Immunofluorescence analysis was performed essentially as previously described [30]. In short, BMDMs were cultured in glass-bottomed dishes at 1.5×10^5 cells/well (0.5 mL) with the complete medium at 37 °C overnight. Cells were primed with 1 μg/mL LPS in

Opti-MEM for 4 h, then were pre-incubated with or without MCC950 (1 μM) for 1 h followed by stimulation with MSU crystals (300 μg/mL) with 6 h in Opti-MEM. After fixation, permeabilization, and blocking, cells were incubated with rabbit anti-p-MLKL antibody (1:300) overnight at 4 °C, followed by staining with CF568-conjugated goat-anti-rabbit IgG and AlexaFluor488-conjugated anti-ASC. In separate experiments staining for ASC alone, cells were incubated with rabbit anti-ASC antibody (1:300) overnight at 4 °C, followed by staining with CF568-conjugated goat-anti-rabbit IgG. Subsequently, nuclei were revealed by Hoechst 33342 staining, the cells were observed under a Zeiss Axio Observer D1 microscope (Carl Zeiss, Göttingen, Germany). Fluorescence images were captured by a Zeiss AxioCam MR R3 cooled CCD camera controlled with ZEN software (Carl Zeiss).

Western blot analysis

Western blotting was performed as previously described [30]. Briefly, proteins were separated by sodium dodecyl sulfate-polyacrylamide gel electrophoresis (SDS-PAGE) and then electrophoretically transferred to PVDF membranes (#03010040001; Roche, Mannheim, Germany). Subsequently, the membranes were blocked in PBS containing 5% non-fat milk powder and 0.1% Tween 20 for 1 h prior to incubation with indicated antibodies overnight at 4 °C, and after washing, membranes were incubated with HRP-conjugated IgG for 1 h at room temperature. After washing, proteins of interest were detected by an enhanced chemiluminescence kit (BeyoECL Plus kit, P0018; Beyotime, Shanghai, China) and X-ray films (Carestream, Xiamen, China). The blot images were captured by the FluorChem8000 imaging system (AlphaInnotech, San Leandro, CA, USA).

Precipitation of soluble proteins

Soluble proteins in culture supernatants were precipitated with 7.2% trichloroacetic acid plus 0.15% sodium deoxycholate as previously reported [30]. The precipitated proteins were re-dissolved in an equal volume of 1 × SDS-PAGE loading buffer and subjected to Western blot analysis of mature IL-1β and caspase-1p10.

ASC oligomer cross-linking

The cross-linking of ASC oligomers was carried out as previously described [28]. Briefly, cells were lysed with cold PBS containing 0.5% Triton X-100, and the cell lysates were centrifuged at 6000 × *g* for 15 min at 4 °C. The pellets were washed twice with PBS and then resuspended in 200 μL PBS and cross-linked with disuccinimidyl suberate (2 mM) for 30 min at room temperature. The cross-linked pellets were centrifuged at 6000 × *g* for 15 min at 4 °C and re-dissolved in 20 μL of 1 × SDS-PAGE sample loading buffer, being subjected to Western blot analysis.

MSU crystal-induced peritonitis

The mouse model of MSU crystal-induced peritonitis was performed essentially as described previously [33]. Mice were administered intragastrically (i.g.) with baicalin (200 mg/kg body weight, which was referred to a previous publication [28]) or vehicle (2% Tween 80 in PBS) once a day for 2 consecutive days prior to intraperitoneal injection with 0.2 mL of sterile PBS alone or with 1 mg MSU crystals (in 0.2 mL sterile PBS). One hour later, mice were treated with vehicle or baicalin (i.g.) once again. After 4 h, mice were sacrificed and peritoneal lavage was performed with 5 mL PBS. The peritoneal lavage fluid was harvested and centrifuged at 300 × *g* for 10 min at 4 °C to remove cells, and the supernatant was collected for the measurement of cytokines. Pelleted cells were analyzed by antibody staining together with flow cytometry.

Flow cytometry analysis

Peritoneal cells were collected by centrifugation and resuspended in 1 mL PBS and the total cell numbers were quantified. Cells were stained with CD11b-FITC and Ly-6G-PE for 30 min at 4 °C. Subsequently, the cells were washed with PBS twice before analysis using a flow cytometer (Attune NxT; ThermoFisher). Neutrophils were identified as $CD11b^{+}Ly\text{-}6G^{+}$ cells. The total number of neutrophils collected from each mouse was calculated by multiplying the percentage of neutrophils with the total cell count acquired.

Determination of soluble cytokines

Soluble cytokines in the peritoneal lavage fluid of mice were determined by cytometric bead array (CBA) mouse IL-1β flex set (#558266) and mouse inflammation kit (#552364) (BD Biosciences, San Jose, CA, USA) according to the manufacturer's instructions. Data were acquired and analyzed with a flow cytometer (Attune NxT).

Statistical analysis

Each experiment was performed three times independently. Data were expressed as mean± standard deviation (SD) and analyzed for statistical significance using GraphPad Prism 6.0 (GraphPad Software Inc, San Diego, CA, USA). One-way analysis of variance (ANOVA) followed by Tukey *post hoc* test and unpaired Student's *t* test was used to analyze the statistical significance among multiple groups and between two groups, respectively. Significance was defined as follows: $^{*}P < 0.05$, $^{**}P < 0.01$, $^{***}P < 0.001$.

RESULTS

MSU crystals induce inflammasome activation and mature IL-1β release dependently on NLRP3 expression

Sufficient activation of NLRP3 inflammasome in murine macrophages needs two activation signals [34]: the first or priming signal converges on the activation of nuclear factor kappa-B (NF-κB) leading to upregulation of both NLRP3 and pro-IL-1β expression, while the second or activating signal, which may be a danger signal (e.g., ATP) or particulate matter (e.g., MSU crystals), can directly induce inflammasome assembly [35]. In this study, we used bacterial lipopolysaccharide (LPS) as the priming signal and MSU crystals as the activating agent to explore NLRP3 inflammasome activation in wild-type (WT) and $NLRP3^{-/-}$ mouse BMDMs. Western blot analysis showed that NLRP3 levels were markedly up-regulated in LPS-primed WT but not $NLRP3^{-/-}$ BMDMs, whereas pro-IL-1β levels were increased in both cell types (Fig. 1a). MSU crystals dose-dependently induced the release of caspase-1p10 (10 kDa) and mature IL-1β (17 kDa), the hallmarks for NLRP3 inflammasome activation, from WT but not from NLRP3-deficient macrophages. In support of the Western blot analysis, CBA assay (with a lower detection limit of 5 pg/mL) also detected significant secretion of IL-1β in WT but not in NLRP3-deficient BMDMs stimulated with MSU crystals (Fig. 1b). Consistent with this, MSU crystals induced the formation of ASC specks in WT but not in $NLRP3^{-/-}$ macrophages (Fig. 1c, d), indicative of NLRP3 inflammasome assembly in WT but not in NLRP3-deficient cells [36]. Besides, we showed that pharmacological inhibition with NLRP3-specific inhibitor MCC950 [37] also efficiently blocked ASC speck formation in WT BMDMs (Fig. 1e, f). Together, these results indicated that MSU crystals had indeed induced the activation of NLRP3 inflammasome and the secretion of mature IL-1β in murine macrophages depending on NLRP3 expression.

MSU crystal-induced necrosis is not reliant on NLRP3 inflammasome activation and caspase-1-mediated GSDMD-NT generation

As active caspase-1 resulting from NLRP3 inflammasome activation can cleave GSDMD to generate GSDMD-NT to execute pyroptosis, a lytic form of cell death [7, 8], we next examined lytic cell death in macrophages treated with MSU crystals.

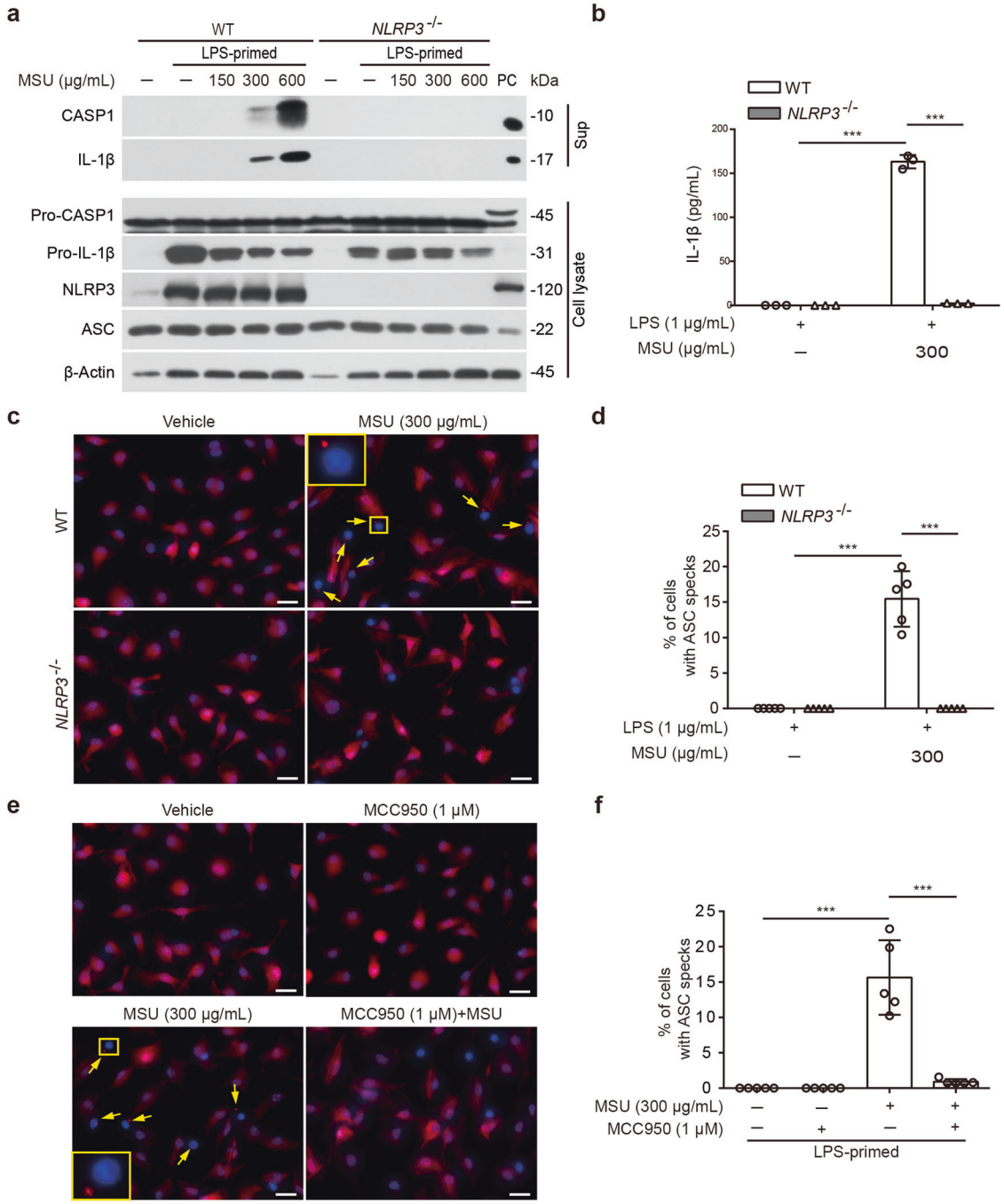

Fig. 1 MSU crystals induce NLRP3 inflammasome activation and IL-1β release. Bone marrow-derived macrophages (BMDMs) from wild-type (WT) and NLRP3-deficient (*NLRP3*$^{-/-}$) mice were primed with lipopolysaccharide (LPS, 1 μg/mL) for 4 h, and then treated with indicated concentrations of monosodium urate (MSU) crystals for 6 h. **a** Western blot analysis was used to assess the expression levels of indicated proteins in cell lysates and culture supernatants. β-Actin was adopted as a loading control for cell lysates. Positive control (PC) was cell lysate from BMDMs primed with LPS (1 μg/mL) for 4 h followed by stimulation with adenosine triphosphate (ATP) (5 mM) for 30 min. **b** The levels of secreted IL-1β in culture supernatants were determined by cytometric bead array (CBA) assay. **c, e** Immunofluorescence microscopy was used to reveal ASC (red) distribution and nuclei (blue, stained by Hoechst 33342). LPS-primed WT BMDMs were pre-treated with or without MCC950 (1 μM, NLRP3 inhibitor) for 1 h, followed by MSU crystals (300 μg/mL) treatment for 6 h (**e**). Yellow arrows indicate ASC specks and enlarged insets show one cell with an ASC speck. Scale bars, 20 μm. **d**, **f** Percentages of cells with an ASC speck relative to total cells from 5 random fields. Data are shown as mean ± SD ($n = 5$). ***$P < 0.001$; CASP1, caspase-1; Pro-CASP1, pro-caspase-1

Unexpectedly, MCC950, a specific inhibitor of NLRP3 activation, did not significantly suppress MSU crystal-induced necrosis as revealed by PI-positive staining (Fig. 2a), although it completely inhibited ASC speck formation (Fig. 1e, f). Besides, caspase-1 inhibitor VX-765 and GSDMD-NT inhibitor disulfiram also showed no inhibitory effects on MSU crystal-induced cell death (Fig. 2b, c). Furthermore, MSU crystals induced similar proportions of PI-positive cells in both WT and NLRP3-deficient BMDMs (Fig. 2d, e), irrespective of the cleavage of GSDMD into GSDMD-NT (32 kDa) (Fig. 2f). In contrast, ATP or nigericin dose-dependently induced necrosis in WT but not in NLRP3-deficient BMDMs (Fig. S1a–f). Consistently, they induced the activation of caspase-1 (as revealed

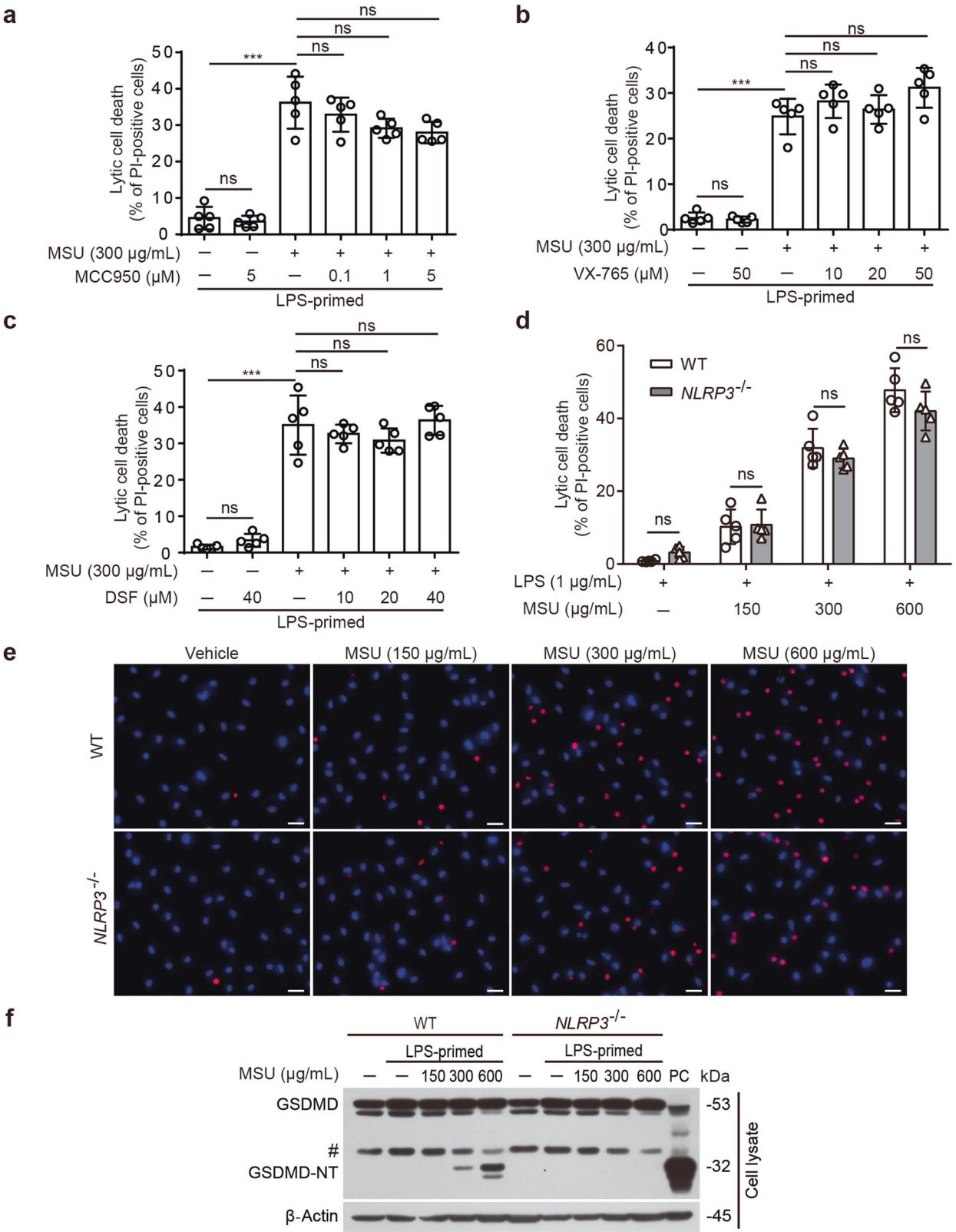

Fig. 2 MSU crystal-induced necrosis does not require the activation of NLRP3 inflammasome. BMDMs were treated as described in Fig. 1. LPS primed cells were pre-treated without or with indicated concentrations of MCC950 (**a**), VX-765 (**b**) (caspase-1 inhibitor), and disulfiram (DSF) (GSDMD inhibitor) (**c**) for 1 h, followed by co-stimulation with MSU crystals (300 μg/mL) for 6 h. Lytic cell death was assessed by propidium iodide (PI) uptake (red, indicating dead cells). PI-positive cells in five randomly chosen fields were quantified in (**a–d**). The percentage of lytic cell death is defined as the ratio of PI-positive cells relative to all cells. Data are shown as mean ± SD ($n = 5$). Representative PI and Hoechst 33342 (blue, indicating all cells) images from wild-type (WT) or *NLRP3*$^{-/-}$ cells captured by fluorescence microscopy are shown in (**e**). Scale bars, 20 μm. **f** GSDMD and GSDMD-NT levels in cell lysates were determined by Western blotting. β-Actin was used as a loading control. #denotes non-specific bands; ***$P < 0.001$, NS not significant

by caspase-1p10 and mature IL-1β release) and cleavage of GSDMD in WT but not in NLRP3-deficient cells (Fig. S2a, b), indicating that such necrosis was NLRP3-dependent pyroptosis while being different from that induced by MSU crystals. Apart from NLRP3, other sensors such as NLRP1, NLRC4, and AIM2 existing in macrophages may also be assembled into inflammasomes leading to caspase-1 activation that can mediate GSDMD cleavage and IL-1β secretion [38, 39]; however, the absence of caspase-1 activation and IL-1β secretion (Fig. 1a, b), as well as GSDMD cleavage (Fig. 2f) in NLRP3-deficient cells suggested that these inflammasomes were not activated by MSU crystals and thus probably not participating in the necrosis. Together, these data suggested that MSU crystal-induced necrosis was independent of the activation of the NLRP3/caspase-1/GSDMD pathway.

The necrosis induced by MSU crystals are partly suppressed by inhibitors for the necroptosis pathway

As the inhibitors for the NLRP3 pathway were ineffective in blocking MSU crystal-induced necrosis, we asked whether those for other cell death-related pathways could suppress the necrosis. It has been reported that phagocytosis of MSU crystals results in lysosomal rapture and production of reactive oxygen species (ROS) [40, 41], and active lysosomal enzymes, such as cathepsin B, are released into the cytosol to trigger NLRP3 inflammasome activation [42, 43]. Furthermore, a large amount of cytosolic cathepsin B can shift the cell death pathway towards necrosis [44], while ROS can cause pyroptosis by inducing NLRP3 activation. Besides, ROS produced by NADPH oxidase (NOX) is known to contribute to NLRP3 inflammasome activation through regulating carnitine palmitoyltransferase 1 A (CPT1A) [45, 46]. We, therefore, utilized CA-074-Me (a cell-permeable analog of CA-074) (cathepsin B inhibitor) and E64d (a cell-permeable pan-cathepsin inhibitor), etomoxir (CPT1A inhibitor), and GKT137831 (NOX1/4 inhibitor) to block the activities of upstream molecules that are involved in NLRP3 inflammasome activation and pyroptosis. PI uptake showed that none of these inhibitors were able to protect BMDMs from MSU crystal-induced necrosis, with CA-074-Me even increasing the cell death (Fig. S3a–f and Fig. S4a, b), indicating that the related pathways had minimal roles in MSU crystal-induced necrosis in macrophages. In addition, we also explored whether ferroptosis or mitochondrial permeability transition (MPT) was the cause of MSU-induced necrosis, but found that neither ferrostatin-1 (a ferroptosis inhibitor) nor cyclosporin A (an MPT-driven necrosis inhibitor) had any inhibitory effects on the necrosis (Fig. S4c–f).

Besides pyroptosis, necroptosis is another form of regulated necrosis that is mediated by RIPK1, RIPK3, and MLKL [47–50]. We next examined whether this form of regulated necrosis had any roles in MSU crystal-induced necrosis. The results showed that although necrostatin-1 (RIPK1 inhibitor) did not have any inhibitory effects (Fig. 3a, b), GSK′872 (RIPK3 inhibitor) or GW806742X (MLKL inhibitor [50]) dose-dependently and significantly suppressed MSU crystal-induced necrosis, respectively (Fig. 3c–f), suggesting that the necrosis appeared to be associated with RIPK3/MLKL-dependent necroptosis. These results together suggested that RIPK3 and MLKL had been involved in MSU crystal-induced necrosis in murine macrophages.

Combined inhibitors for multiple signaling pathways can markedly suppress MSU crystal-induced necrosis

Considering that multiple cell death pathways can be activated simultaneously in macrophages as reported recently [21], we presumed that a combination of cell death pathway inhibitors might display enhanced suppression of MSU crystal-induced necrosis. To test this, we assayed MSU crystal-induced lytic cell death in both WT and *NLRP3*$^{-/-}$ macrophages pre-treated with different combinations of cell death inhibitors. In WT macrophages, IDN-6556 (pan-caspase inhibitor) plus GSK′872 showed a similar inhibitory effect to that of GW806742X (MLKL inhibitor [50]) alone, while the triple combination (IDN-6556 + GSK′872 + GW806742X) showed a slightly enhanced effect (Fig. 4a, c). Notably, the addition of MCC950 to the triple combination markedly enhanced the inhibitory effect, although MCC950 only slightly enhanced the effect of GW806742X or unexpectedly even attenuated the inhibitory effect of IDN-6556 plus GSK′872 in WT cells. Similar results were obtained from *NLRP3*$^{-/-}$ macrophages, but MCC950 showed minimal effects on the triple combination or GW806742X in NLRP3-deficient cells (Fig. 4b, d). In addition, neither CA-074-Me nor E64d had any influences on the inhibitory effects of GSK′872 or GSK′872 plus GW806742X (Figs. S5a–d and S6a–d), suggesting that cathepsins, including cathepsin B and L, were not obviously involved in the necrosis. Interestingly, there were no significant differences in necrosis between WT and *NLRP3*$^{-/-}$ macrophages when pre-treated with various inhibitor combinations except that addition of MCC950 to IDN-6556 plus GSK′872 or the triple combination (IDN-6556 + GSK′872 + GW806742X) showed differential inhibitory effects (the reason is unclear at present) (Fig. S7). Together, these results indicated that multiple cell death pathways had contributed to MSU crystal-induced necrosis, suggesting that combined inhibitor regimens may be potential pro-drugs for blocking such necrosis.

Phosphorylation of MLKL in macrophages treated with MSU crystals is independent of NLRP3 inflammasome activation

As MSU crystal-induced necrosis was suppressed by combined inhibitors for multiple signaling pathways, we next biochemically determined whether other cell death pathways beyond NLRP3 inflammasome had been activated. Western blotting showed that MSU crystals did not activate caspase-9, caspase-8, and caspase-3 and were also unable to induce cleavage of GSDME and PARP (two substrates for caspase-3) in both WT and *NLRP3*$^{-/-}$ macrophages (Fig. S8a), suggesting that apoptotic caspases and secondary necrosis were not involved in the necrosis. Although it could not inhibit the necrosis (Fig. 2a), MCC950 entirely blocked not only the release of caspase-1p10 and mature IL-1β (17 kDa) but also the cleavage of GSDMD (Fig. 5a), which as consistent with the blockade of NLRP3 inflammasome activation (Fig. 1e, f), suggesting that GSDMD cleavage was not necessary for MSU crystal-induced necrosis. In line with this notion, IDN-6556 plus GSK′872 was able to markedly suppress the necrosis (Fig. 4a, c) but only partially attenuated GSDMD cleavage (Fig. 5a). Unexpectedly, GW806742X, an established MLKL inhibitor, was able to entirely block not only the release of caspase-p10 and mature IL-1β (17 kDa) but also the cleavage of GSDMD (Fig. 5a), indicating that it had effectively suppressed the activation of NLRP3 inflammasome induced by MSU crystals. Similarly, the other combinations that contained either MCC950 or GW806742X were also able to entirely block NLRP3 inflammasome activation (Fig. 5a).

Although necroptosis inhibitors including MLKL inhibitor (GW806742X) and RIPK3 inhibitor (GSK′872) significantly inhibited MSU crystal-induced necrosis, we were unable to detect phosphorylated MLKL (p-MLKL) by Western blotting (Fig. S8b). So we presumed that MSU crystals might have weakly or subcellularly induced the phosphorylation of MLKL in macrophages. Indeed, immunofluorescence microscopy revealed that p-MLKL was observed in the cells treated with MSU crystals, with the p-MLKL fluorescence being largely around the crystals but not with ASC speck in WT cells (Fig. 5b). Moreover, neither MCC950 nor NLRP3 deficiency blocked MSU crystal-induced phosphorylation of MLKL in the cells, even though both treatments blocked ASC speck formation (Fig. 5b, c). These results indicated that apart from pyroptosis, the necroptosis signaling pathway had been triggered in macrophages by MSU crystals independently of NLRP3 inflammasome activation.

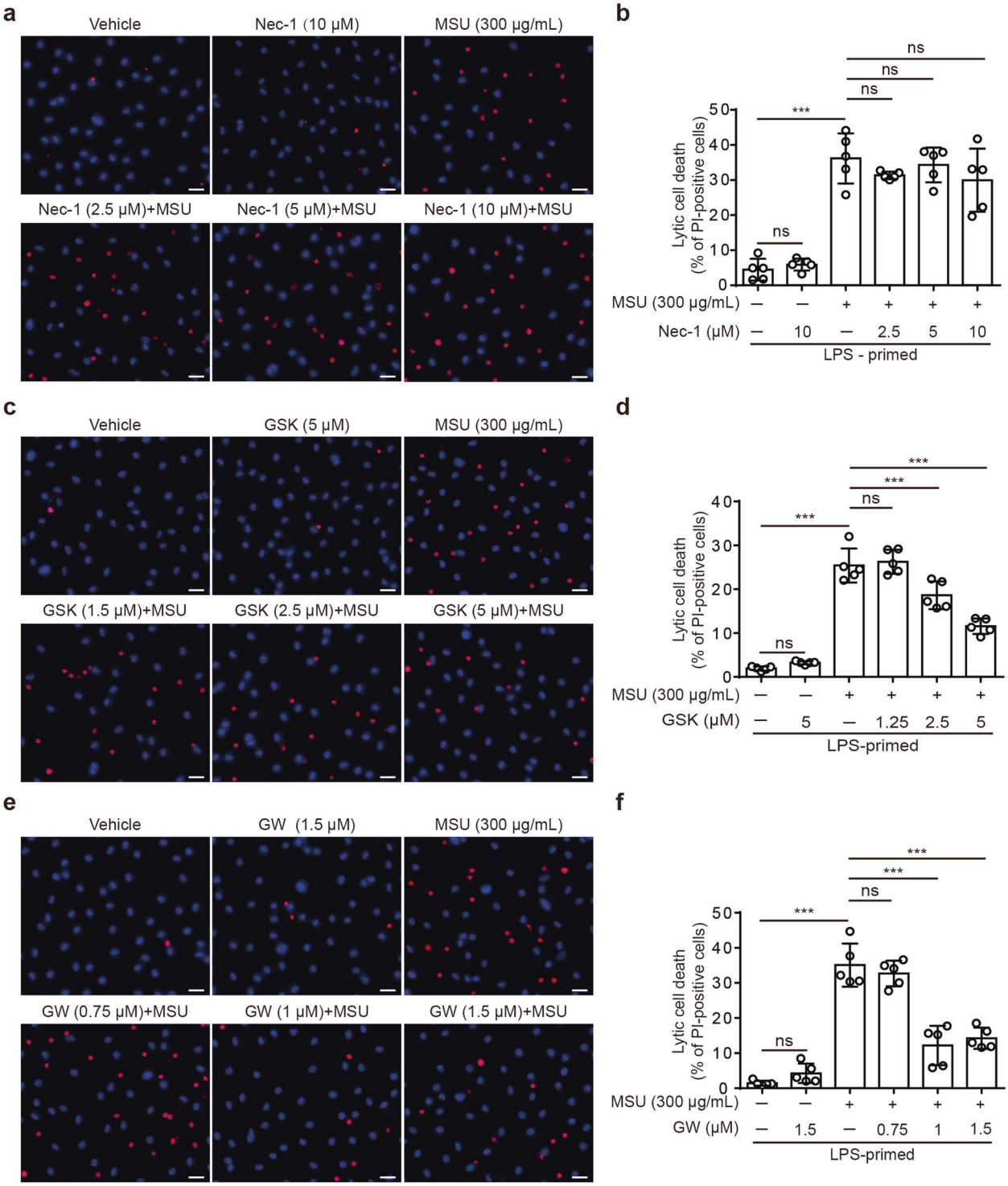

Fig. 3 MSU crystal-induced necrosis can be partly suppressed by inhibitors for the necroptosis pathway. BMDMs from WT mice were first primed with LPS (1 μg/mL), then pre-treated without or with gradient doses of necrostatin-1 (Nec-1, RIPK1 inhibitor), GSK′872 (GSK, RIPK3 inhibitor), or GW806742X (GW, MLKL inhibitor) for 1 h, followed by stimulation with MSU crystals (300 μg/mL) for 6 h in the presence or absence of indicated inhibitors. Lytic cell death was measured by PI staining. **a**, **c,** and **e** Fluorescence microscopy was adopted to capture images with PI (red, staining dead cells) and Hoechst 33342 fluorescence (blue, staining all nuclei), Scale bars, 20 μm. **b**, **d,** and **f** The ratio of PI-positive cells was quantified. Data are shown as mean ± SD ($n = 5$). ***$P < 0.001$, NS not significant.

Baicalin significantly inhibits not only NLRP3 inflammasome activation but also the necrosis in macrophages treated with MSU crystals

Apart from the combination of the synthetic inhibitors, we asked whether natural products isolated from traditional medicinal herbs with known anti-inflammatory activities could suppress MSU crystal-induced necrosis. One candidate is baicalin, which has been previously shown to inhibit ATP or nigericin-induced NLRP3 inflammasome activation in murine macrophages [28]. To test its effects on MSU crystal-induced inflammasome activation,

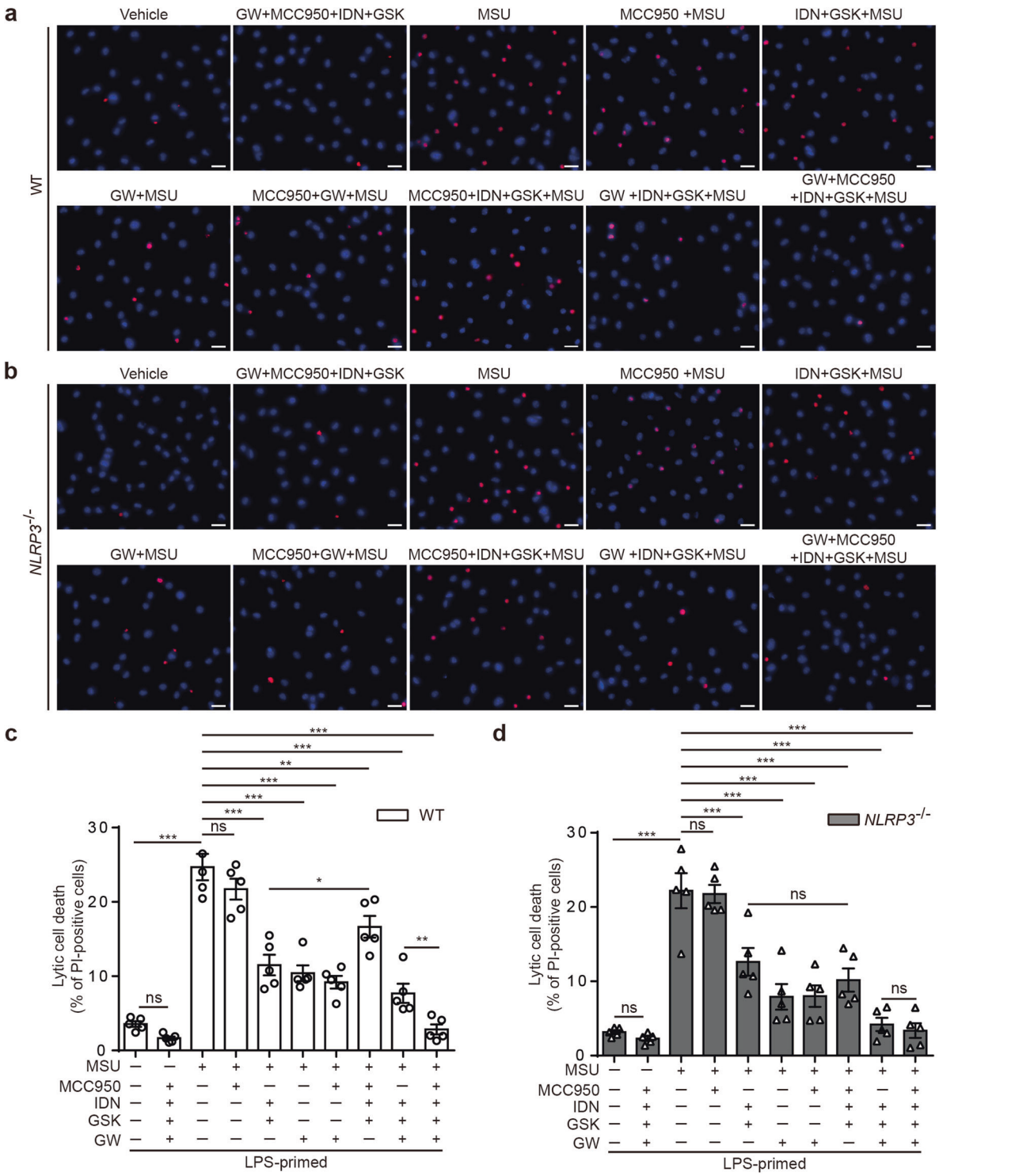

Fig. 4 Combination of multiple signaling pathway inhibitors can markedly suppress MSU crystal-induced necrosis in murine macrophages. BMDMs from WT and *NLRP3*$^{-/-}$ mice were primed with LPS (1 μg/mL) for 4 h, and then pre-incubated without or with single or combination of multiple signaling pathway inhibitors for 1 h, followed by co-treatment with MSU crystals (300 μg/mL) for 6 h. **a**, **b** Representative lytic cell death images captured by fluorescence microscopy show PI (red, staining dead cells) combined with Hoechst 33342 (blue, staining all nuclei). Scale bars, 20 μm. **c**, **d** Quantitative percentage of PI-positive cells in **a** and **b**, respectively. Data are shown as mean ± SD ($n = 5$). *$P < 0.05$; **$P < 0.01$; ***$P < 0.001$, NS not significant. MCC950 (NLRP3 inhibitor, 1 μM), IDN-6556 (IDN, pan-caspase inhibitor, 20 μM), GSK'872 (GSK, RIPK3 inhibitor, 5 μM) and GW806742X (GW) (MLKL inhibitor, 1 μM) were used alone or in different combinations

we performed both Western blotting and cytokine assay. The results showed that baicalin was able to inhibit the release of caspase-1p10 and mature IL-1β (17 kDa) into culture supernatants in a dose-dependent manner (Fig. 6a). CBA assay confirmed similar inhibition of IL-1β secretion (Fig. 6b). Cross-linking test also revealed that MSU crystal-induced ASC oligomerization (indicative of inflammasome assembly) was suppressed by baicalin (Fig. 6c). These data together indicated

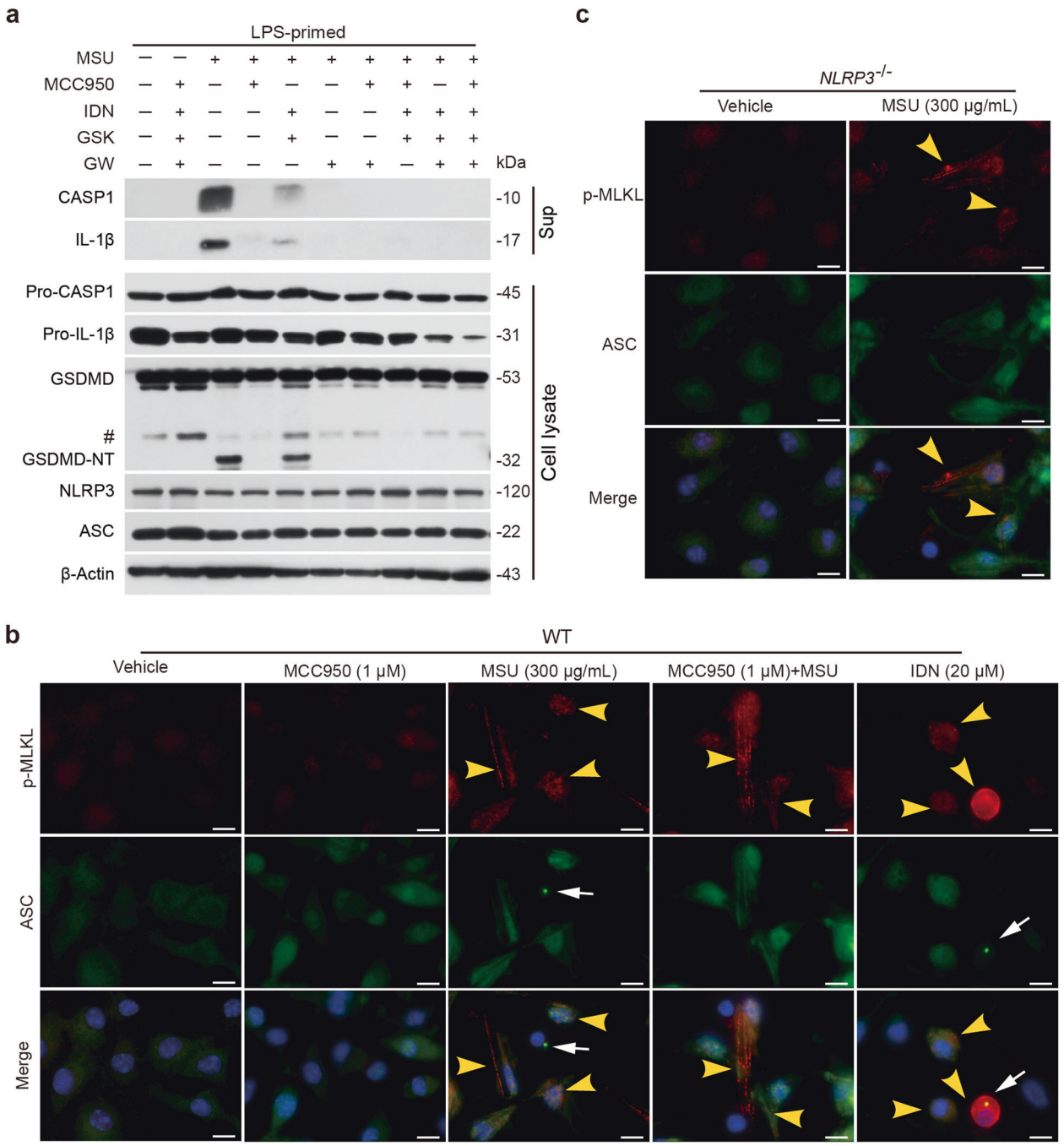

Fig. 5 p-MLKL is detected in macrophages treated with MSU crystals independent of NLRP3 inflammasome activation. BMDMs from WT and *NLRP3*$^{-/-}$ mouse were primed with LPS (1 μg/mL) for 4 h and then pre-treated with one or a combination of multiple death pathway inhibitors for 1 h, followed by MSU (300 μg/mL) co-stimulation for 6 h. **a** Western blot analysis was used to detect the expression levels of indicated proteins in cell lysates and culture supernatants (Sup). β-Actin was used as a protein-loading control. **b** Immunofluorescence microscopy showing the distribution of p-MLKL (red) and ASC (green) while nuclei (blue) being revealed by Hoechst 33342 staining. IDN-6556 (IDN) (20 μM) alone was used to trigger necroptosis as a positive control. **c** Analysis of p-MLKL and ASC distribution in *NLRP3*$^{-/-}$ BMDMs. White arrows and yellow arrowheads were respectively used to indicate ASC specks and p-MLKL fluorescence. Scale bars, 10 μm. #denotes non-specific bands.

that baicalin was able to inhibit MSU crystal-induced activation of NLRP3 inflammasome.

We next tested the effect of baicalin on MSU crystal-induced necrosis. LDH release assay revealed that MSU crystal-induced release of LDH into the culture medium, indicative of lytic cell death (necrosis), was dose-dependently inhibited by pre-treatment with baicalin (Fig. 6d). Consistent with this, the PI uptake assay also revealed that baicalin dose-dependently suppressed the necrosis (Fig. 6e, f). In addition, in human THP-1-derived macrophages treated with MSU crystals, baicalin pre-treatment not only inhibited IL-1β release (indicative of NLRP3 inflammasome activation) but also suppressed the necrosis (Fig. S9a–c), although the cells appeared not much sensitive to MSU crystal treatment in that only low levels of PI-positive cells were observed (Fig. S9b, c). Together, these results

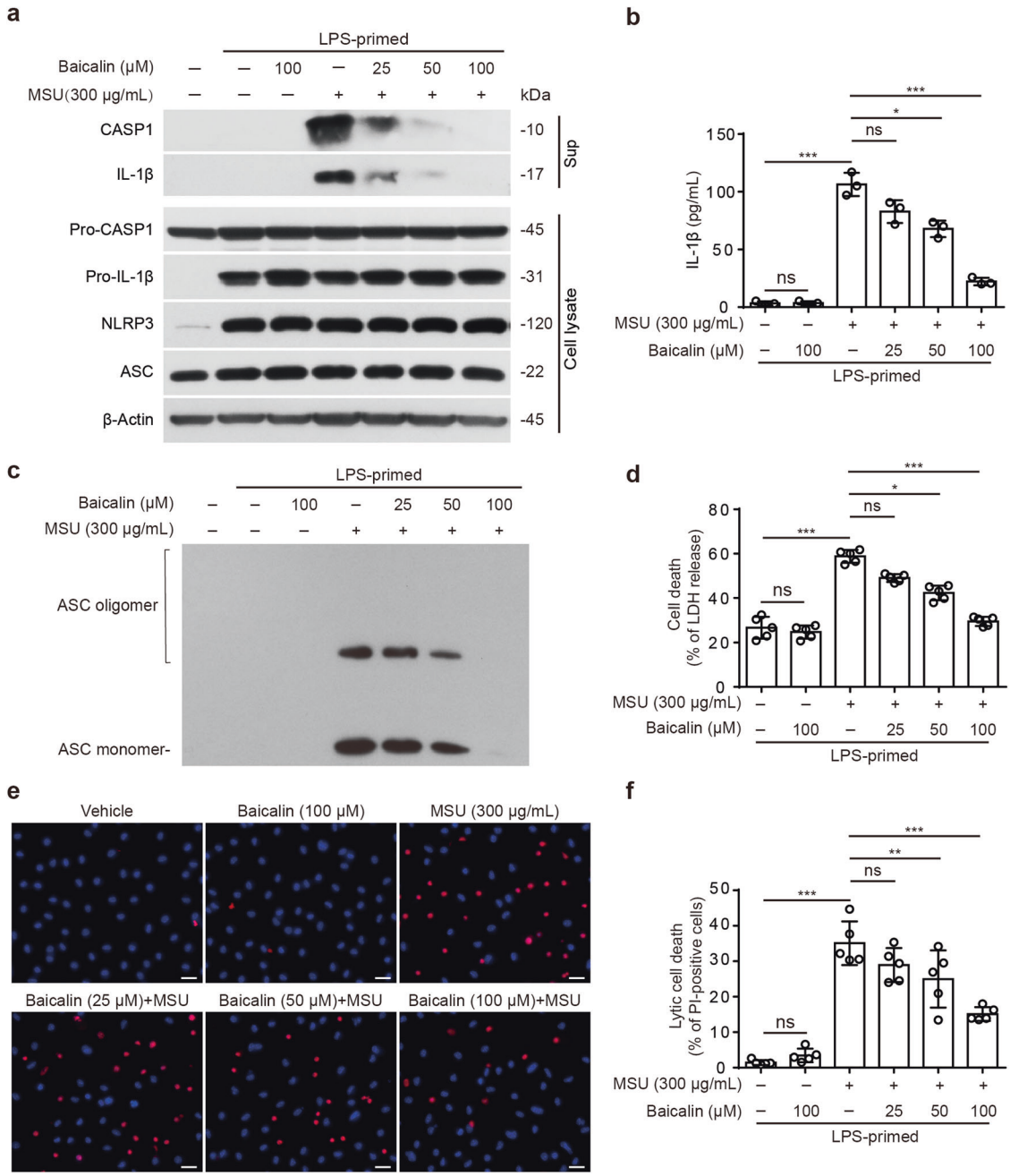

Fig. 6 Baicalin significantly inhibits not only NLRP3 inflammasome activation but also the necrosis in macrophages treated with MSU crystals. BMDMs from WT mice were primed with LPS (1 μg/mL) for 4 h, and then pre-treated without or with graded doses of baicalin for 1 h, followed by stimulation with MSU crystals (300 μg/mL) for 6 h in the presence or absence of baicalin. **a** The expression levels of indicated proteins in cell lysates and culture supernatants (Sup) were analyzed by Western blotting. β-Actin was adopted as a loading control for cell lysates. **b** The levels of secreted IL-1β in culture supernatants were determined by cytometric bead array (CBA). **c** Western blotting analysis of ASC oligomers in Triton X-100 insoluble pellets cross-linked with disuccinimidyl suberate. **d** Lytic cell death was measured by lactic acid dehydrogenase (LDH) release in culture supernatants ($n = 5$). **e** Representative images showing PI (red, staining dead cells) combined with Hoechst 33342 (blue, staining all cells) fluorescence. Scale bars, 20 μm. **f** Quantification of PI-positive cells in 5 randomly chosen fields and ratio of PI-positive over all cells (revealed by Hoechst 33342) is defined as the percentages of lytic cell death. Data are shown as mean± SD ($n = 5$). *$P < 0.05$; **$P < 0.01$; ***$P < 0.001$, NS not significant.

indicated that the natural product baicalin not only inhibited NLRP3 inflammasome activation but also suppressed necrosis in macrophages upon MSU crystal treatment.

Baicalin significantly inhibits MSU crystal-induced peritonitis in mice

Considering that administration of combined inhibitors in vivo needs careful selection of a proper dose for each inhibitor, we tested the in vivo effect of baicalin on MSU crystal-induced peritonitis (a murine peritoneal model of acute gout) in mice. The results showed that baicalin administration via gavage significantly reduced the recruitment of neutrophils in the peritoneal cavity of mice receiving an intraperitoneal injection of MSU crystals (Fig. 7a–c). Besides, the levels of both IL-1β and IL-6 in the peritoneal lavage fluids were significantly decreased by baicalin treatment in comparison to a vehicle (Fig. 7d, e).

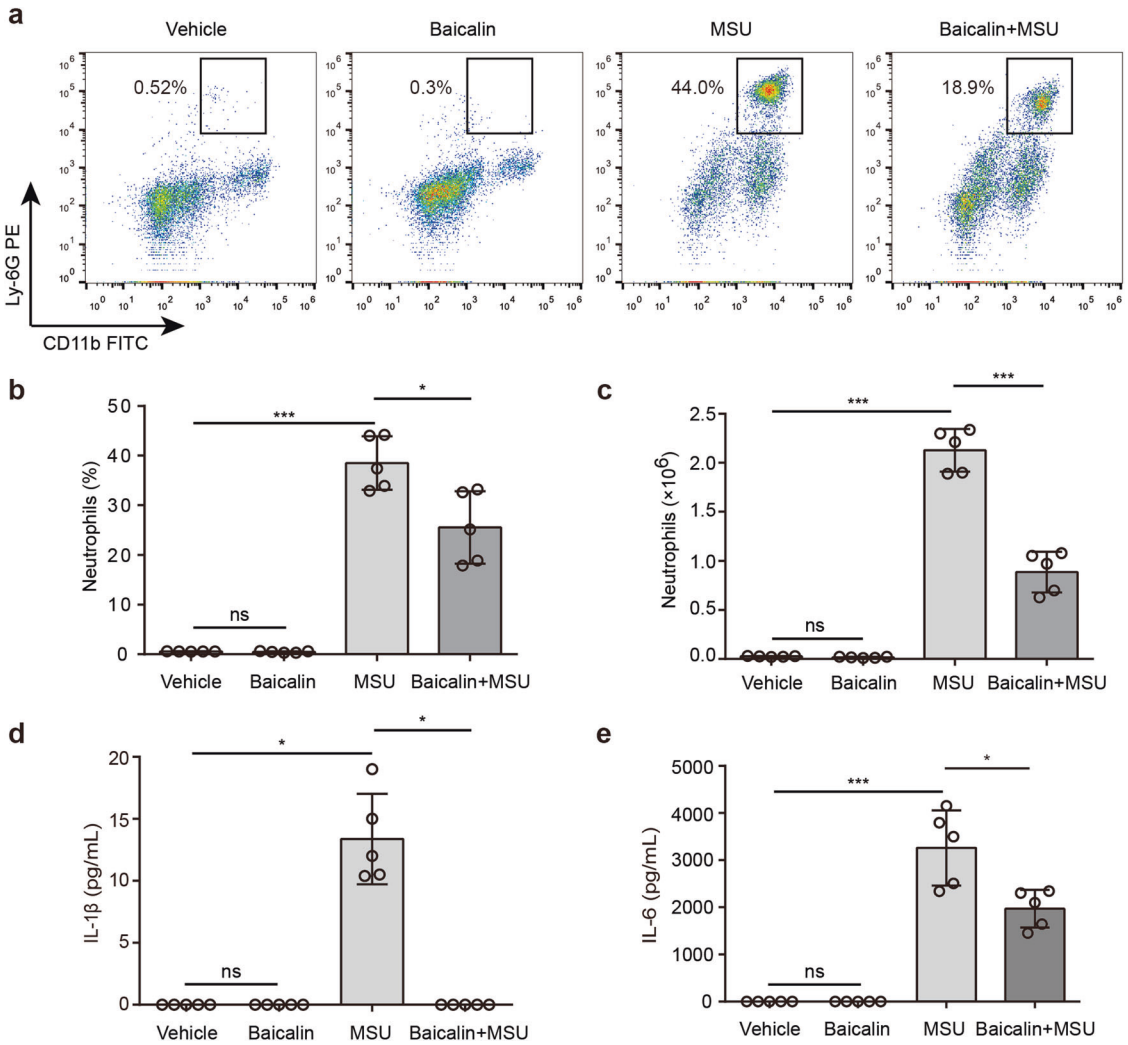

Fig. 7 MSU crystal-induced peritonitis can be ameliorated by baicalin gavage. C57BL/6 J mice were administered intragastrically (i.g.) with baicalin (200 mg/kg body weight) or vehicle (2% Tween 80 in PBS) once a day for 2 consecutive days prior to intraperitoneal injection with sterile PBS (0.2 mL) or with 1 mg MSU crystals (in 0.2 mL sterile PBS). One hour later, mice were administered with vehicle or baicalin (i.g.) once again. Neutrophil and soluble cytokine levels in the peritoneal lavage fluids were quantified 4 h after MSU crystal administration ($n = 5$ mice per group). **a** Representative flow cytometric dot-plots of peritoneal exudate cells. **b, c** Quantification of neutrophils in peritoneal lavage fluids. **d, e** IL-1β and IL-6 levels in peritoneal lavage fluid supernatants were measured by cytometric bead array (CBA) assay. Data are shown as mean ± SD ($n = 5$). *$P < 0.05$, ***$P < 0.001$.

These results indicated that baicalin had dampened MSU crystal-induced peritonitis in mice.

DISCUSSION

MSU crystals not only trigger the activation of NLRP3 inflammasome and release of mature IL-1β but also induce regulated necrosis [5, 15, 16], both of which have been shown to play critical roles in the initiation and pathogenesis of gouty arthritis [2–4]. However, inflammasome activation-mediated pyroptosis appears not to be solely responsible for MSU crystal-induced necrosis because blocking NLRP3 inflammasome-mediated pyroptosis has minimal effects on cell death [15]. Thus what forms of regulated necrosis have been induced by MSU crystals is unclear, while the inhibitors for MSU crystal-induced necrosis remain to be explored. We showed in this study that MSU crystal-induced necrosis was not significantly suppressed by individual NLRP3 pathway inhibitors including MCC950 (NLRP3 inhibitor), VX-765 (caspase-1 inhibitor), and disulfiram (GSDMD inhibitor [51]), consistent with previous studies [15]. Unexpectedly, we found that some necroptosis pathway inhibitors, such as GSK′872 (RIPK3 inhibitor) and GW806742X (MLKL inhibitor [50]), at least partly, suppressed MSU crystal-induced necrosis. Although IDN-6556 (pan-caspase inhibitor) alone increased the necrosis due to induction of necroptosis, it did enhance the inhibitory effects when combined with GSK′872 and GW806742X. When MCC950 was administered in combination with the triple regimen composed of IDN-6556, GSK′872, and GW806742X, they displayed the strongest inhibitory effects on the necrosis in both wild-type and NLRP3-deficient macrophages. Our data indicated that multiple forms of regulated necrosis, including NLRP3-mediated pyroptosis, had been induced by MSU crystals in murine macrophages.

Our finding that combined inhibitors, instead of individuals, showed the strongest inhibitory effect on MSU crystal-induced necrosis reveals a possibility that the necrosis involves multiple forms of regulated necrosis. This notion is supported by several previous studies. For example, it has been shown that GSDMD was rapidly cleaved in macrophages treated with MSU crystals indicating induction of pyroptosis and that GSDMD deletion could not prevent MSU crystal-induced necrosis [15]. It has also

been demonstrated that MSU crystals and other particulate matters can induce different forms of necrosis such as pyroptosis, necroptosis, ferroptosis, and MPT-driven necrosis, thus leading to necroinflammation; such auto-amplifying loop between inflammation and necrosis could lead to disease state called crystallopathies [4]. Recently identified PANoptosis is an example of simultaneous induction of pyroptosis, apoptosis, and necroptosis by a variety of pathogens [18–22], suggesting induction of multiple forms of necrosis is not limited to particulate matters like MSU crystals. Meanwhile, our own data also support the notion for induction of multiple forms of regulated necrosis: firstly, we observed that GSDMD-NT, an executor of pyroptosis, was induced by MSU crystals, indicating induction of pyroptotic cell death; secondly, blocking the NLRP3/caspase-1/GSDMD pathway had no significant inhibitory effects on MSU crystal-induced necrosis; thirdly, combined inhibitors for pyroptosis, apoptosis, and necroptosis had the strongest inhibitory effects on the necrosis. Yet, the exact cell death mechanisms behind MSU crystal-induced necrosis remain to be clarified in future research.

Even though NLRP3 deficiency or individual pharmacological inhibitors did not significantly suppress the necrosis in this study, the role of NLRP3 inflammasome-mediated pyroptosis in MSU crystal-induced necrosis cannot be completely ruled out. One reason is that MSU crystals indeed induced generation of GSDMD-NT that can execute pyroptosis. As blocking NLRP3-mediated pyroptosis has been shown to switch cell death to caspase-3/GSDME-mediated secondary necrosis in macrophages [32], the ineffectiveness of NLRP3 inhibitor MCC950 or GSDMD inhibitor disulfiram [51] alone may be explained by a switch to other forms of regulated necrosis. Indeed, the addition of MCC950 to the triple regimen (IDN-6556, GSK′872, and GW806742X) could further enhance the inhibitory effect on the necrosis in wild-type but not in NLRP3-deficient cells (Fig. 4c, d). Thus, NLRP3 inhibitor in combination with apoptosis and necroptosis inhibitors may represent a new regimen for the treatment of gouty arthritis.

One interesting finding is that GW806742X alone displayed a marked inhibitory effect on MSU crystal-induced necrosis. As GW806742X has been discovered to be an inhibitor of pseudokinase MLKL to suppress necroptosis [50], this seems inconsistent with a previous study showing that genetic deletion of MLKL does not block MSU crystal-induced necrosis [15]. One possible explanation is that GW806742X might have also inhibited RIPK1 and RIPK2 activities due to its off-target effect [52]. Besides, MLKL protein inhibited by GW806742X might act as a scaffolding to prevent necrosis whereas MLKL deletion abrogates such a possibility. The third possibility may be also associated with its off-target effects on the NLRP3 inflammasome pathway as evidenced by full inhibition of caspase-1p10 and mature IL-1β release as well as GSDMD-NT generation (Fig. 5a), suggesting that GW806742X had blocked both pyroptosis and necroptosis pathways. Yet this notion still awaits further clarification.

Although it could enhance the inhibitory effects of triple combination (IDN-6556, GSK′872, and GW806742X) in wild-type macrophages, MCC950 attenuated the inhibitory effect of IDN-6556 plus GSK′872 on wild-type but not on NLRP3-deficient cells. There are two possible explanations for this phenomenon: one is that binding of MCC950 to NLRP3 might have triggered or promoted another as-yet-unknown form of cell death that may be blocked by GW806742X; the other is that MCC950-blocked NLRP3 protein might have acted as a scaffolding to counteract the effects of IDN-6556 in combination with GSK′872. More investigations are warranted to explore these hypotheses.

Baicalin is a major anti-inflammatory ingredient in various medicinal herbs [27] and has been identified as an inhibitor for ATP or nigericin-induced NLRP3 inflammasome activation [28]. Consistent with the previous study, we found that baicalin was able to effectively inhibit MSU crystal-induced NLRP3 inflammasome activation. Importantly, whereas MCC950 (as a potent NLRP3-specific inhibitor [37]) did not inhibit MSU crystal-induced necrosis, baicalin significantly inhibited the necrosis in murine macrophages, suggesting that baicalin is a potential drug for inhibiting MSU crystal-induced inflammation in vivo. Indeed, in a murine model of peritoneal acute gout (MSU crystal-induced peritonitis), baicalin effectively inhibited neutrophil influx into the peritoneal cavity and markedly suppressed the levels of pro-inflammatory cytokines including IL-1β and IL-6. Besides, baicalin also suppressed MSU crystal-induced necrosis and IL-1β release in human THP-1-derived macrophages, suggesting its translational relevance. Thus, baicalin warrants future research for the treatment of gouty arthritis.

It is still unclear how MSU crystals induce necrosis in macrophages. As our data show induction of multiple forms of regulated necrosis, it is possible that multi-action mechanisms may have been involved. For example, cathepsins (including cathepsin B) released from disrupted lysosomes have been shown to play critical roles in NLRP3 inflammasome activation induced by MSU crystals [42]. Although we found in this study that cathepsin B and pan-cathepsin inhibitors have no obvious inhibitory effects on MSU crystal-induced necrosis, the role of the lysosome in this process cannot be completely excluded. Recently, it has been reported that the Rag-Ragulator on the lysosome can serve as a platform for activating a FADD-RIPK1-caspase-8 complex to trigger pyroptosis in response to Toll-like receptor and tumor necrosis factor receptor (TNFR) ligation [53]. Thus, one possibility is that an as-yet-unknown signaling pathway on the lysosome might have been activated by MSU crystals leading to necrosis. Besides, phagocytosis of MSU crystals by macrophages may also induce damages to other organelles such as the mitochondrion leading to necrosis because the mitochondrion is a central hub for governing multiple forms of cell death.

In summary, we revealed that MSU crystals were able to induce multiple forms of regulated necrosis independently of the NLRP3 pathway and that such necrosis was effectively suppressed by a combination of inhibitors for pyroptosis, apoptosis, and necroptosis or by the natural product baicalin. Baicalin administration via gavage significantly ameliorated MSU crystal-induced peritonitis in a mouse model of acute gout. Our data highlight that targeting MSU crystal-induced necrosis by a combined inhibitor regimen or other multi-target drugs may be a potential avenue to treat gouty arthritis.

ACKNOWLEDGEMENTS

This work was supported by the National Natural Science Foundation of China (81773965, 81873064, and 81673664).

AUTHOR CONTRIBUTIONS

CSZ, BZ, JHQ, and MYZ performed cellular experiments; LHX, YTH, RX, and SYL performed animal experiments; XHH, QBZ, and CSZ designed the research; CSZ and BZ analyzed the data; XHH, DYOY, and BH wrote the paper.

ADDITIONAL INFORMATION

Supplementary information The online version contains supplementary material available at https://doi.org/10.1038/s41401-021-00749-7.

Competing interests: The authors declare no competing interests.

REFERENCES

1. Dalbeth N, Merriman TR, Stamp LK. Gout. Lancet. 2016;388:2039–52.
2. Desai J, Steiger S, Anders HJ. Molecular pathophysiology of gout. Trends Mol Med. 2017;23:756–68.
3. Dalbeth N, Choi HK, Joosten LAB, Khanna PP, Matsuo H, Perez-Ruiz F, et al. Gout. Nat Rev Dis Prim. 2019;5:69.
4. Mulay SR, Anders HJ. Crystallopathies. N Engl J Med. 2016;374:2465–76.

5. Martinon F, Pétrilli V, Mayor A, Tardivel A, Tschopp J. Gout-associated uric acid crystals activate the NALP3 inflammasome. Nature. 2006;440:237–41.
6. So A, Dumusc A, Nasi S. The role of IL-1 in gout: from bench to bedside. Rheumatol (Oxf). 2018;57:i12–i19.
7. Shi J, Zhao Y, Wang K, Shi X, Wang Y, Huang H, et al. Cleavage of GSDMD by inflammatory caspases determines pyroptotic cell death. Nature. 2015;526:660–5.
8. He WT, Wan H, Hu L, Chen P, Wang X, Huang Z, et al. Gasdermin D is an executor of pyroptosis and required for interleukin-1β secretion. Cell Res. 2015;25:1285–98.
9. Liu X, Zhang Z, Ruan J, Pan Y, Magupalli VG, Wu H, et al. Inflammasome-activated gasdermin D causes pyroptosis by forming membrane pores. Nature. 2016;535:153–8.
10. Ding J, Wang K, Liu W, She Y, Sun Q, Shi J, et al. Pore-forming activity and structural autoinhibition of the gasdermin family. Nature. 2016;535:111–6.
11. Sborgi L, Rühl S, Mulvihill E, Pipercevic J, Heilig R, Stahlberg H, et al. GSDMD membrane pore formation constitutes the mechanism of pyroptotic cell death. Embo J. 2016;35:1766–78.
12. Shi J, Gao W, Shao F. Pyroptosis: gasdermin-mediated programmed necrotic cell death. Trends Biochem Sci. 2017;42:245–54.
13. Kovacs SB, Miao EA. Gasdermins: effectors of pyroptosis. Trends Cell Biol. 2017; 27:673–84.
14. Galluzzi L, Vitale I, Aaronson SA, Abrams JM, Adam D, Agostinis P, et al. Molecular mechanisms of cell death: recommendations of the Nomenclature Committee on Cell Death 2018. Cell Death Differ. 2018;25:486–541.
15. Rashidi M, Simpson DS, Hempel A, Frank D, Petrie E, Vince A, et al. The pyroptotic cell death effector gasdermin D is activated by gout-associated uric acid crystals but is dispensable for cell death and IL-1β release. J Immunol. 2019;203:736–48.
16. Mulay SR, Desai J, Kumar SV, Eberhard JN, Thomasova D, Romoli S, et al. Cytotoxicity of crystals involves RIPK3-MLKL-mediated necroptosis. Nat Commun. 2016;7:10274.
17. Linkermann A, Stockwell BR, Krautwald S, Anders HJ. Regulated cell death and inflammation: an auto-amplification loop causes organ failure. Nat Rev Immunol. 2014;14:759–67.
18. Christgen S, Zheng M, Kesavardhana S, Karki R, Malireddi RKS, Banoth B, et al. Identification of the PANoptosome: a molecular platform triggering pyroptosis, apoptosis, and necroptosis (PANoptosis). Front Cell Infect Microbiol. 2020;10:237.
19. Malireddi RKS, Kesavardhana S, Karki R, Kancharana B, Burton AR, Kanneganti TD. RIPK1 distinctly regulates Yersinia-induced inflammatory cell death. PANoptosis Immunohorizons. 2020;4:789–96.
20. Zheng M, Williams EP, Malireddi RKS, Karki R, Banoth B, Burton A, et al. Impaired NLRP3 inflammasome activation/pyroptosis leads to robust inflammatory cell death via caspase-8/RIPK3 during coronavirus infection. J Biol Chem. 2020;295:14040–52.
21. Malireddi RKS, Kesavardhana S, Kanneganti TD. ZBP1 and TAK1: master regulators of NLRP3 inflammasome/pyroptosis, apoptosis, and necroptosis (PAN-optosis). Front Cell Infect Microbiol. 2019;9:406.
22. Place DE, Lee S, Kanneganti TD. PANoptosis in microbial infection. Curr Opin Microbiol. 2021;59:42–9.
23. Fritsch M, Günther SD, Schwarzer R, Albert MC, Schorn F, Werthenbach JP, et al. Caspase-8 is the molecular switch for apoptosis, necroptosis and pyroptosis. Nature. 2019;575:683–7.
24. Newton K, Wickliffe KE, Maltzman A, Dugger DL, Reja R, Zhang Y, et al. Activity of caspase-8 determines plasticity between cell death pathways. Nature. 2019;575: 679–82.
25. Orning P, Weng D, Starheim K, Ratner D, Best Z, Lee B, et al. Pathogen blockade of TAK1 triggers caspase-8-dependent cleavage of gasdermin D and cell death. Science. 2018;362:1064–9.
26. Li Y, Song K, Zhang H, Yuan M, An N, Wei Y, et al. Anti-inflammatory and immunomodulatory effects of baicalin in cerebrovascular and neurological disorders. Brain Res Bull. 2020;164:314–24.
27. Dinda B, Dinda S, DasSharma S, Banik R, Chakraborty A, Dinda M. Therapeutic potentials of baicalin and its aglycone, baicalein against inflammatory disorders. Eur J Med Chem. 2017;131:68–80.
28. Li CG, Yan L, Mai FY, Shi ZJ, Xu LH, Jing YY, et al. Baicalin Inhibits NOD-like receptor family, pyrin containing domain 3 Inflammasome activation in murine macrophages by augmenting protein kinase A signaling. Front Immunol. 2017;8:1409.
29. Shu JX, Zhong CS, Shi ZJ, Zeng B, Xu LH, Ye JZ, et al. Berberine augments hypertrophy of colonic patches in mice with intraperitoneal bacterial infection. Int Immunopharmacol. 2021;90:107242.
30. Ye J, Zeng B, Zhong M, Li H, Xu L, Shu J, et al. Scutellarin inhibits caspase-11 activation and pyroptosis in macrophages via regulating PKA signaling. Acta Pharm Sin B. 2021;11:112–26.
31. Py BF, Jin M, Desai BN, Penumaka A, Zhu H, Kober M, et al. Caspase-11 controls interleukin-1β release through degradation of TRPC1. Cell Rep. 2014;6:1122–8.
32. Zeng CY, Li CG, Shu JX, Xu LH, Ouyang DY, Mai FY, et al. ATP induces caspase-3/gasdermin E-mediated pyroptosis in NLRP3 pathway-blocked murine macrophages. Apoptosis. 2019;24:703–17.
33. Magupalli VG, Negro R, Tian Y, Hauenstein AV, Di Caprio G, Skillern W, et al. HDAC6 mediates an aggresome-like mechanism for NLRP3 and pyrin inflammasome activation. Science. 2020;369:eaas8995. https://doi.org/10.1126/science.aas8995.
34. Broz P, Dixit VM. Inflammasomes: mechanism of assembly, regulation and signalling. Nat Rev Immunol. 2016;16:407–20.
35. Franchi L, Muñoz-Planillo R, Núñez G. Sensing and reacting to microbes through the inflammasomes. Nat Immunol. 2012;13:325–32.
36. Man SM, Kanneganti TD. Regulation of inflammasome activation. Immunol Rev. 2015;265:6–21.
37. Coll RC, Robertson AA, Chae JJ, Higgins SC, Muñoz-Planillo R, Inserra MC, et al. A small-molecule inhibitor of the NLRP3 inflammasome for the treatment of inflammatory diseases. Nat Med. 2015;21:248–55.
38. Bergsbaken T, Fink SL, Cookson BT. Pyroptosis: host cell death and inflammation. Nat Rev Microbiol. 2009;7:99–109.
39. Evavold CL, Kagan JC. Inflammasomes: threat-assessment organelles of the innate immune system. Immunity. 2019;51:609–24.
40. Maejima I, Takahashi A, Omori H, Kimura T, Takabatake Y, Saitoh T, et al. Autophagy sequesters damaged lysosomes to control lysosomal biogenesis and kidney injury. Embo J. 2013;32:2336–47.
41. Castelblanco M, Lugrin J, Ehirchiou D, Nasi S, Ishii I, So A, et al. Hydrogen sulfide inhibits NLRP3 inflammasome activation and reduces cytokine production both in vitro and in a mouse model of inflammation. J Biol Chem. 2018;293:2546–57.
42. Campden RI, Zhang Y. The role of lysosomal cysteine cathepsins in NLRP3 inflammasome activation. Arch Biochem Biophys. 2019;670:32–42.
43. Chevriaux A, Pilot T, Derangère V, Simonin H, Martine P, Chalmin F, et al. Cathepsin B is required for NLRP3 inflammasome activation in macrophages, through NLRP3 interaction. Front Cell Dev Biol. 2020;8:167.
44. Talukdar R, Sareen A, Zhu H, Yuan Z, Dixit A, Cheema H, et al. Release of cathepsin B in cytosol causes cell death in acute pancreatitis. Gastroenterology. 2016;151: 747–58.e745.
45. O'Leary DP, Wang JH, Cotter TG, Redmond HP. Less stress, more success? oncological implications of surgery-induced oxidative stress. Gut. 2013;62:461–70.
46. Moon JS, Nakahira K, Chung KP, DeNicola GM, Koo MJ, Pabón MA, et al. NOX4-dependent fatty acid oxidation promotes NLRP3 inflammasome activation in macrophages. Nat Med. 2016;22:1002–12.
47. Sun L, Wang H, Wang Z, He S, Chen S, Liao D, et al. Mixed lineage kinase domain-like protein mediates necrosis signaling downstream of RIP3 kinase. Cell. 2012; 148:213–27.
48. Chen X, Li W, Ren J, Huang D, He WT, Song Y, et al. Translocation of mixed lineage kinase domain-like protein to plasma membrane leads to necrotic cell death. Cell Res. 2014;24:105–21.
49. Wang H, Sun L, Su L, Rizo J, Liu L, Wang LF, et al. Mixed lineage kinase domain-like protein MLKL causes necrotic membrane disruption upon phosphorylation by RIP3. Mol Cell. 2014;54:133–46.
50. Hildebrand JM, Tanzer MC, Lucet IS, Young SN, Spall SK, Sharma P, et al. Activation of the pseudokinase MLKL unleashes the four-helix bundle domain to induce membrane localization and necroptotic cell death. Proc Natl Acad Sci USA. 2014;111:15072–7.
51. Hu JJ, Liu X, Xia S, Zhang Z, Zhang Y, Zhao J, et al. FDA-approved disulfiram inhibits pyroptosis by blocking gasdermin D pore formation. Nat Immunol. 2020;21:736–45.
52. Yan B, Liu L, Huang S, Ren Y, Wang H, Yao Z, et al. Discovery of a new class of highly potent necroptosis inhibitors targeting the mixed lineage kinase domain-like protein. Chem Commun. 2017;53:3637–40.
53. Zheng Z, Deng W, Bai Y, Miao R, Mei S, Zhang Z, et al. The lysosomal rag-ragulator complex licenses RIPK1– and caspase-8–mediated pyroptosis by Yersinia. Science. 2021;372:eabg0269. https://doi.org/10.1126/science.abg0269.